



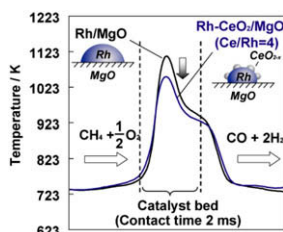
## Contents

### REGULAR ARTICLES

#### Catalytic performance and characterization of Rh–CeO<sub>2</sub>/MgO catalysts for the catalytic partial oxidation of methane at short contact time

pp 1–8

Hisanori Tanaka, Rie Kaino, Kazu Okumura, Tokushi Kizuka, Keiichi Tomishige\*

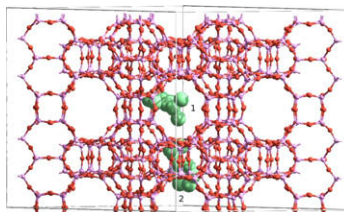


The addition of CeO<sub>2</sub> to Rh/MgO decreased the catalyst bed temperature in the catalytic partial oxidation of methane and this property will contribute to the suppression of hot spot formation.

#### The benefit of multipore zeolites: Catalytic behaviour of zeolites with intersecting channels of different sizes for alkylation reactions

pp 9–17

Avelino Corma\*, Francisco J. Llopis, Cristina Martínez, Germán Sastre, Susana Valencia

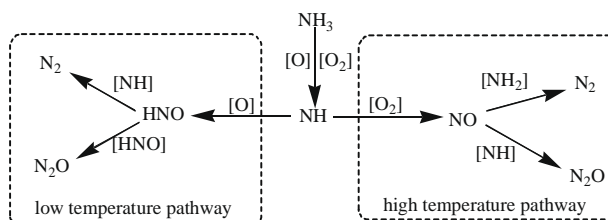


Two multipore zeolites, ITQ-22 and SSZ-33, have been studied as catalysts for the alkylation of benzene to ethylbenzene and cumene. Whereas SSZ-33, which could be seen as a zeolite with 12 MR “cavities” connected by 10 and 12 MR, presents an intermediate behaviour as compared to ZSM-5 and Beta, zeolite ITQ-22 shows a unique behaviour as a multipurpose alkylation catalyst, close to that of the medium pore ZSM-5 in the case of alkylation with ethanol, and close to the large pore Beta for alkylation with isopropanol or propylene. These results are discussed on the basis of its particular topology and on the location of the acidic protons as determined by means of a computational study.

#### Mechanism of selective catalytic oxidation of ammonia to nitrogen over Ag/Al<sub>2</sub>O<sub>3</sub>

pp 18–25

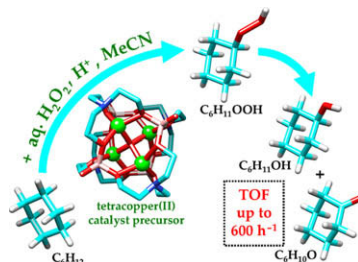
Li Zhang, Hong He\*



Scheme illustrating the pathways of NH<sub>3</sub>–O<sub>2</sub> reaction over Ag/Al<sub>2</sub>O<sub>3</sub>.

**Remarkably fast oxidation of alkanes by hydrogen peroxide catalyzed by a tetracopper(II) triethanolamine complex: Promoting effects of acid co-catalysts and water, kinetic and mechanistic features** pp 26–38

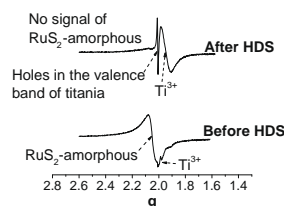
Marina V. Kirillova, Yuriy N. Kozlov, Lidia S. Shul'pina, Oleg Y. Lyakin, Alexander M. Kirillov, Evgenii P. Talsi, Armando J.L. Pombeiro\*, Georgiy B. Shul'pin\*



Kinetic and mechanistic features of mild alkane oxidations with a tetracopper(II) catalyst and an acid promoter are studied, revealing remarkably fast cyclohexane oxidation in the presence of HCl and unusual rate-accelerating role of water.

**Spectroscopic study of the electronic interactions in Ru/TiO<sub>2</sub> HDS catalysts** pp 39–48

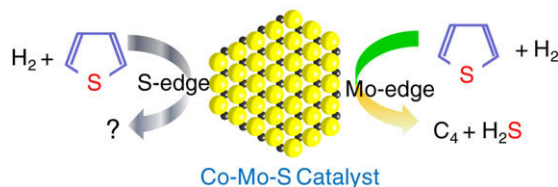
Perla Castillo-Villalón, Jorge Ramírez\*



The HDS activity trend of Ru/TiO<sub>2</sub> with sulfidation temperature is explained by electronic interactions between the TiO<sub>2</sub> support and the Ru phases present on the surface (Ru<sup>0</sup> and RuS<sub>2</sub>-pyrite).

**Effect of sulfidation atmosphere on the hydrodesulfurization activity of SiO<sub>2</sub>-supported Co–Mo sulfide catalysts: Local structure and intrinsic activity of the active sites** pp 49–59

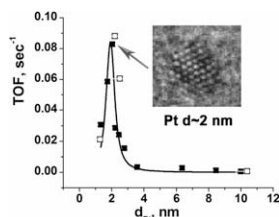
Yasuaki Okamoto\*, Kazuya Hioka, Kenichi Arakawa, Takashi Fujikawa, Takeshi Ebihara, Takeshi Kubota



The intrinsic activity of Co–Mo–S for HDS is strongly dependent on its location and local structure as well as on the MoS<sub>2</sub>-support interactions.

**Platinum nanoparticles on Al<sub>2</sub>O<sub>3</sub>: Correlation between the particle size and activity in total methane oxidation** pp 60–67

Irene E. Beck\*, Valerii I. Bukhtiyarov, Ilya Yu. Pakharukov, Vladimir I. Zaikovskiy, Vladimir V. Kriventsov, Valentin N. Parmon

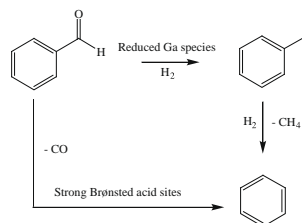


Catalytic activity of size-controlled platinum nanoparticles supported on the acid-pretreated  $\gamma$ -alumina has been measured in complete methane oxidation under lean conditions. The strong size sensitivity was shown to originate from the size dependence of the apparent activation energy of the methane oxidation and/or oxidation state of platinum in the catalytically active nanoparticles.

**Catalytic deoxygenation of benzaldehyde over gallium-modified ZSM-5 zeolite**

pp 68–78

Artit Ausavasukhi, Tawan Sooknoi, Daniel E. Resasco \*

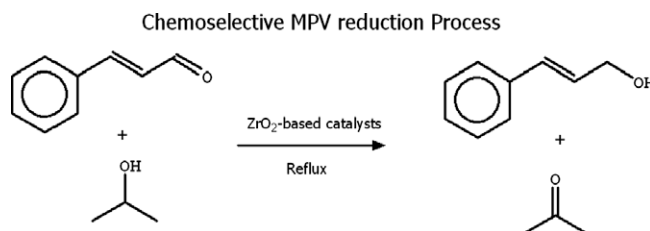


The deoxygenation of benzaldehyde over gallium-modified ZSM-5 catalysts results in two main products benzene and toluene, depending on the reaction conditions and pretreatment. In the absence of hydrogen, Ga/HZSM-5 catalyzes benzaldehyde decarbonylation resulting in benzene with CO as a side product. By contrast, when hydrogen is present, toluene (plus water) is the dominant product produced over reduced gallium sites by hydrogenation/hydrogenolysis. The formation of benzene and methane via dealkylation of toluene represents only a small contribution compared to the production of benzene via decarbonylation.

**An insight into the Meerwein–Ponndorf–Verley reduction of  $\alpha,\beta$ -unsaturated carbonyl compounds: Tuning the acid–base properties of modified zirconia catalysts**

pp 79–88

Francisco J. Urbano \*, María A. Aramendía, Alberto Marinas, José M. Marinas

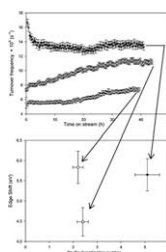


Pure and modified ZrO<sub>2</sub> catalysts were used in the Meerwein–Ponndorf–Verley reduction of cinnamaldehyde with 2-propanol. The most active sites are seemingly Brønsted acid sites of medium–high strength formed by doping ZrO<sub>2</sub> with boron. Modifying ZrO<sub>2</sub> with an alkaline-earth metal enhances its basicity, thereby reducing its catalytic activity although increasing its selectivity for the unsaturated alcohol.

**Rhenium complexes and clusters supported on  $\gamma$ -Al<sub>2</sub>O<sub>3</sub>: Effects of rhenium oxidation state and rhenium cluster size on catalytic activity for *n*-butane hydrogenolysis**

pp 89–99

Rodrigo J. Lobo-Lapidus, Bruce C. Gates \*

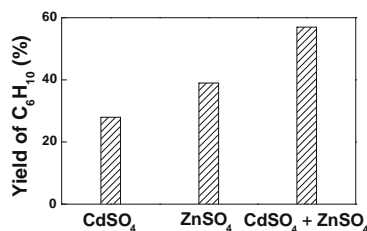


A family of  $\gamma$ -Al<sub>2</sub>O<sub>3</sub>-supported clusters of rhenium allowed resolution of the effects of cluster size and rhenium oxidation state on catalytic activity for *n*-butane conversion with H<sub>2</sub>.

**Discrimination of the roles of CdSO<sub>4</sub> and ZnSO<sub>4</sub> in liquid phase hydrogenation of benzene to cyclohexene**

pp 100–105

Jian-Liang Liu, Yuan Zhu, Jun Liu, Yan Pei, Zhen Hua Li \*, Hui Li, He-Xing Li, Ming-Hua Qiao \*, Kang-Nian Fan

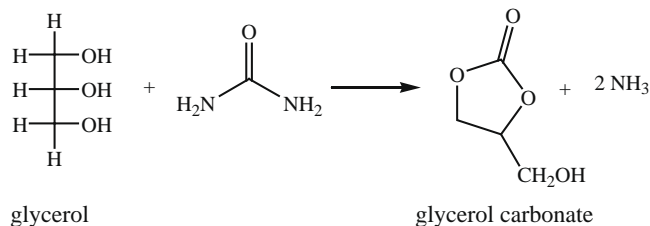


CdSO<sub>4</sub> and ZnSO<sub>4</sub> act as co-modifiers for RuLa/SBA-15 catalyst to enhance the selectivity in the partial hydrogenation of benzene to cyclohexene suppressing re-adsorption and stabilizing cyclohexene, respectively.

**Valorization of bio-glycerol: New catalytic materials for the synthesis of glycerol carbonate via glycerolysis of urea**

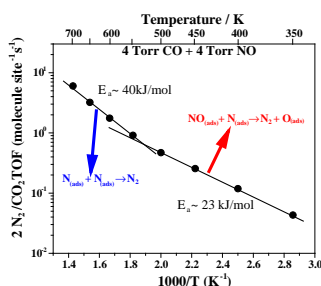
pp 106–114

Michele Aresta \*, Angela Dibenedetto, Francesco Nocito, Carla Ferragina

Glycerolysis of urea with  $\gamma$ -ZrP, a heterogeneous catalyst, is an efficient route to glycerol carbonate.**CO/NO and CO/NO/O<sub>2</sub> reactions over a Au–Pd single crystal catalyst**

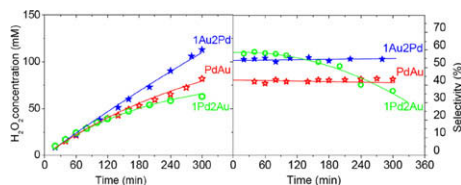
pp 115–121

Feng Gao, Yilin Wang, D. Wayne Goodman \*

CO + NO = CO<sub>2</sub> + 1/2N<sub>2</sub> reaction undergoes almost stoichiometrically on AuPd(1 0 0) with two kinetic regimes. Considerable reaction rate is achieved below ~500 K due mainly to reduced CO/NO inhibition.**Influence of the preparation method on the morphological and composition properties of Pd–Au/ZrO<sub>2</sub> catalysts and their effect on the direct synthesis of hydrogen peroxide from hydrogen and oxygen**

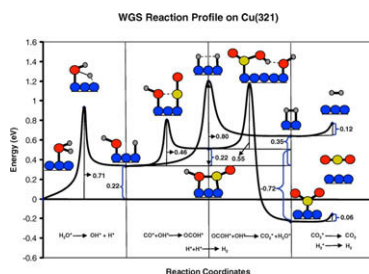
pp 122–130

Federica Menegazzo, Michela Signoretto, Maela Manzoli, Flora Boccuzzi, Giuseppe Cruciani, Francesco Pinna, Giorgio Strukul \*

The preparation method of Pd–Au/zirconia catalysts strongly influences H<sub>2</sub>O<sub>2</sub> direct synthesis. Au changes the chemical composition of the metallic particles, their morphology, and charge of the exposed Pd sites.**Influence of step sites in the molecular mechanism of the water gas shift reaction catalyzed by copper**

pp 131–141

José L.C. Fajín, M. Natália D.S. Cordeiro, Francesc Illas \*, José R.B. Gomes \*

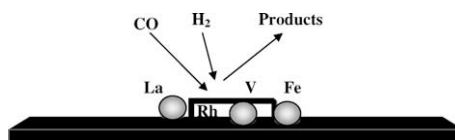


The effect of the surface steps in the mechanism of the water gas shift reaction catalyzed by Cu surfaces has been studied by means of periodic density functional calculations using the stepped Cu(3 2 1) surface as a realistic model of the catalyst surface. The calculations show that the reaction will proceed following the associative mechanism through the carboxyl intermediate with carboxyl dehydrogenation assisted by adsorbed OH.

**La, V, and Fe promotion of Rh/SiO<sub>2</sub> for CO hydrogenation: Detailed analysis of kinetics and mechanism**

pp 142–149

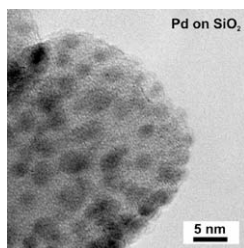
Jia Gao, Xunhua Mo, James G. Goodwin Jr. \*



Investigation of the kinetics for CO hydrogenation on La-, V-, and Fe-promoted SiO<sub>2</sub>-supported Rh showed that the use of different promoters results in different rate-limiting steps.

**Kinetics and particle size effects in ethene hydrogenation over supported palladium catalysts at atmospheric pressure** pp 150–155

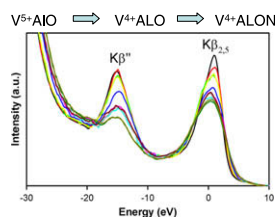
Axel Binder \*, Martin Seipenbusch, Martin Muhler, Gerhard Kasper



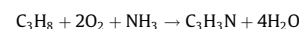
Ethene hydrogenation catalyzed by narrowly size-distributed Pd catalysts, produced by CVD, was investigated. A pronounced size dependence of TOF was found with a maximum at 3–4 nm.

**Local environment of vanadium in V/Al/O-mixed oxide catalyst for propane ammoxidation: Characterization by *in situ* valence-to-core X-ray emission spectroscopy and X-ray absorption spectroscopy** pp 156–164

O.V. Safonova, M. Florea, J. Bilde, P. Delichere, J.M.M. Millet \*



Ammoxidation of propane

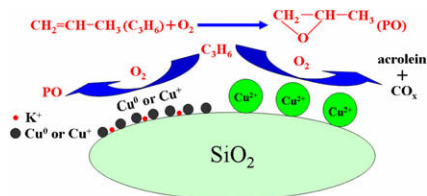


*In situ* valence-to-core X-ray emission and X-ray absorption spectroscopies at V K-edge of V/Al/O catalysts showed that their activation on-stream was associated with reduction of vanadium in the bulk structure and nitridation only on the surface.

**A molecular insight into propylene epoxidation on Cu/SiO<sub>2</sub> catalysts using O<sub>2</sub> as oxidant**

pp 165–174

Weiguang Su, Shouguo Wang, Pinliang Ying, Zhaochi Feng, Can Li \*



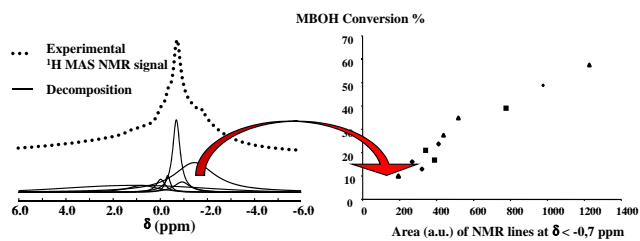
Cu<sup>0</sup> and Cu<sup>+</sup> species in small CuO particles modified by potassium acetate can catalyze C<sub>3</sub>H<sub>6</sub> epoxidation by O<sub>2</sub> much efficiently. However, Cu<sup>2+</sup> species mainly produces acrolein and CO<sub>x</sub>.

## RESEARCH NOTE

Identification of the OH groups responsible for kinetic basicity on MgO surfaces by  $^1\text{H}$  MAS NMR

pp 175–179

Céline Chizallet, Hugo Petitjean, Guylène Costentin, H  l  ne Lauron-Pernot\*, Jocelyne Maquet, Christian Bonhomme, Michel Che



Hydroxylated MgO surfaces are very efficient as base catalysts.  $^1\text{H}$  MAS NMR characterization shows that the OH groups at  $\delta < -0.7$  ppm are the active basic sites in the model reaction of 2-methyl-3-butyn-2-ol conversion. From theoretical studies, they are assigned to low coordinated  $\text{O}_1\text{C}\text{H}$  and  $\text{O}_2\text{C}\text{H}$ .